

## **General Disclaimer**

### **One or more of the Following Statements may affect this Document**

- This document has been reproduced from the best copy furnished by the organizational source. It is being released in the interest of making available as much information as possible.
- This document may contain data, which exceeds the sheet parameters. It was furnished in this condition by the organizational source and is the best copy available.
- This document may contain tone-on-tone or color graphs, charts and/or pictures, which have been reproduced in black and white.
- This document is paginated as submitted by the original source.
- Portions of this document are not fully legible due to the historical nature of some of the material. However, it is the best reproduction available from the original submission.

(NASA-TM-78982) MEASUREMENT OF TRANSIENT  
STRAIN AND SURFACE TEMPERATURE ON SIMULATED  
TURBINE BLADES USING NONCONTACTING  
TECHNIQUES (NASA) 18 p HC A02/MF A01

N79-19415

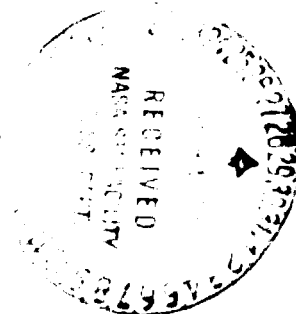
Unclass  
18741

CSCI 20K G3/39

MEASUREMENT OF TRANSIENT STRAIN AND SURFACE  
TEMPERATURE ON SIMULATED TURBINE BLADES  
USING NONCONTACTING TECHNIQUES

Frederick D. Calfo and Frank G. Pollack  
Lewis Research Center  
Cleveland, Ohio

August 1978



## SUMMARY

Noncontacting techniques were used to measure strain and surface temperature of thermally cycled simulated turbine blades. The blades were subjected to cyclic heating (3 minutes) and cooling (1 minute) by moving them into and out of a Mach 1 hot gas stream so that metal temperatures ranging from 300 K (80 °F) to 1300 K (1880 °F) were obtained. The strain measurement technique employed a commercially available noncontacting electro-optical extensometer to measure transient displacement between parallel platinum-rhodium wire targets which were mounted on the blade leading edge. An infrared photographic (IRP) pyrometer method was used to measure surface temperature. An error of less than 1% in specific temperature measurements was obtained and temperature difference measurements over the surface were accurate within 3 K (5 °F). Leading edge strain and steady state surface temperature distribution were obtained for blades of three different configurations, uncooled solid, convection with local film cooling, and convection cooled. Calibration measurements showed the extensometer could measure the displacement to  $\pm 0.04\%$  of the gage length (the distance between the targets.) Strain results were reproducible within 4%. IRP pyrometry showed gross variations of surface temperature distribution for the differently cooled blades. The blade cooled by convection showed the lowest spread of temperatures as well as the smallest temperature gradients across the mid span.

E-9180

## INTRODUCTION

The objective of this program was to develop and demonstrate the capability of using noncontacting techniques for measuring the strain at a critical location of a structural component such as a turbine blade, as well as the entire surface temperature distribution as a function of time (i.e., as a component is subjected to its entire heating and cooling cycle). This capability will be used to fulfill one of the objectives of the fatigue research being conducted at the Lewis Research Center; namely, the development and evaluation of life prediction methods which would be applicable to aircraft gas turbine engine components such as blades and vanes. The component life

prediction studies at Lewis are discussed in references 1-7. These studies include: (1) development of life prediction methods for potential failure modes, and (2) evaluation of these methods by various rig studies using specimens that simulate engine components.

This report describes the use of a commercially available noncontacting electro-optical extensometer system for measuring the transient thermal strain at the mid-span leading edge of simulated turbine blades of three different cooling configurations. In addition, a noncontacting infrared photographic (IRP) pyrometry system was used to acquire the entire surface temperature distributions of these same simulated turbine blades for the steady state temperature test conditions.

Turbine engine designers are required to determine the design life of components in advance of service. Basic input for life prediction are the strain history and temperature at the critical location of the component. The strain history is computed by using the geometry, material properties, and very often, an assumed temperature history based on previous experience. This procedure leads to obvious uncertainties and approximations based on the input assumptions. All possible sources of inaccuracies must be separated out when attempting to verify a life prediction method. Accurate measurement of strain and temperature at the critical location of the component, is one way of reducing the uncertainties in fatigue life prediction of simulated turbine blades. A comparison of predicted life with the measured life as determined in a test facility can then be used to evaluate the effectiveness of the life prediction method.

A noncontacting technique (reference 8) was used to measure leading edge strain of a simulated blade in a test rig because the high test temperature and high gas stream velocity were not appropriate for the use of simpler measuring methods. Leading edge strain was measured during the complete heating and cooling cycle. This required the strain measuring instrument to follow the specimen through the complete thermal cycle.

The strain measuring technique was capable of measuring the displacement between two 0.15 cm (0.060 in) platinum-rhodium wire targets mounted on the edge of the simulated turbine blade. The blade was alternately moved from the exhaust gas stream of a Mach 1 combustion unit to an ambient air stream. The system was designed to measure the change in length between the two targets nominally 1.3 cm (0.50 in) apart, with an accuracy of  $\pm 5$  micrometers ( $\pm 200$  microinches) at a working distance not less than 15 cm (6.0 in). The ratio of the displacement at temperature

to the distance between the targets (gage length) at room temperature gave the strain.

An infrared photographic (IRP) pyrometry method (reference 9) was used to measure the heated steady state surface temperature distribution on the simulated turbine blades. This optical method combines the principles of radiation pyrometry and photography. All surfaces emit radiation as a function of their absolute temperature and photography is used to record the surface radiance distribution within a narrow bandwidth. A thermal image of a heated turbine blade is first formed on film and processed. The film density distribution is converted into a temperature distribution with a suitable calibration procedure. This method provides steady state temperature measurements over a considerable area of the turbine blade with high spatial resolution.

In this investigation the developments described above were applied to simulated turbine blades of three configurations, uncooled solid, convection with local film cooling, and convection cooled. The blades were moved into and out of a high velocity hot gas stream to simulate the thermal fatigue loading experienced by blades in aircraft gas turbines. Each blade was held in a Mach 1 gas stream for three minutes and then moved out for one minute so that metal temperatures ranging from 300 K (80 °F) to 1300 K (1880 °F) were obtained.

## NONCONTACT MEASURING TECHNIQUES

### Transient Strain Measurement

A noncontacting extensometer was used to measure leading edge strain (mechanical plus free thermal expansion) over a 1.3 cm (0.5 in) gage length of a simulated turbine blade during transient heating and cooling. The technique was employed to measure the displacement between two platinum-rhodium targets mounted at right angles to the leading edge of the blade.

A block diagram of the electro-optical extensometer system is shown in figure 1(a). The extensometer consists of an optical head and related electronic modules. The optical head (1) containing lenses and mirrors together with an image analyzer section was used to produce a split optical image of each target. This split optical image was translated to an electrical output directly proportional to the position of each target at any given time. The function of the electronic control module (2) is to provide voltages

corresponding to the targets' relative position in the field of view. A differential amplifier (3) accepts the output signal and provides an analog voltage proportional to the relative displacement of the targets on the turbine blades. This voltage was monitored with an oscilloscope (4) and recorded on a strip chart (5). The ratio of the displacement at temperature to the distance between the targets at room temperature provides the strain. Calibration is required to relate relative displacement to absolute values. This was done by simulating a target change by using the calibration controls provided on the electro-optical extensometer. This noncontacting technique to experimentally determine strain is fully described in reference 8.

### Surface Temperature Distribution Measurement

The IRP pyrometry method used in this investigation is shown in the block diagram in figure 1(b). The system consists of a remotely controlled camera (1) to image the blade radiation through an IR filter onto IR sensitive film; a film processor (2); a microdensitometer (3) to measure and record film density information over the entire thermal image; and a computer (4) provided with calibration data to calculate the temperature distribution from the film density record. The system provides a turbine blade temperature record (5) consisting of temperature profiles and two-dimensional contour maps of temperature distribution.

The calibration technique is described in detail in reference 9. A brief description follows: An area of each film is exposed with a calibrated relative energy scale (step tablet or gray scale). The exposure determines the film response curve. The film response curve is then correlated with a temperature distribution curve. This latter curve is the distribution of relative radiant energy with temperature and is a plot of Planck's equation integrated over the bandwidth of detection. The latter is determined by the IR filter transmission factor and the IR film spectral sensitivity. The optical pyrometer shown in the diagram of figure 1(b) was used to obtain a reference temperature at the time the thermal photograph was taken. This reference point was used to correlate the two curves and provide a calibrated temperature range from a measured film density range. The absolute accuracy of IRP pyrometry technique is determined by a number of factors, the major one being the accuracy of the measured reference temperature. With reasonable care, an error of less than 1% can be obtained, and temperature difference measurements over the surface are accurate to within 3 K (5 °F).

## TEST APPARATUS AND PROCEDURE

### Test Specimens

Three turbine blade configurations were investigated. One was uncooled, another was cooled convection with local film cooling, and the third was convection cooled. These simulated turbine blades were precision cast from a nickel base alloy B-1900 and are illustrated in figure 2.

The convectively cooled blades with local film cooling, were cooled by air entering through both platens (upper and lower) and exiting by way of the leading edge holes and trailing edge slots. The convection cooled blades were internally cooled by air entering the upper platen and exiting through the lower platen.

### Facility Description

A schematic of the facility used for thermal fatigue testing of the simulated turbine blades is shown in figure 3. The rig consists of a Mach 1 burner using natural gas fuel, and a hydraulic loading fixture. The loading fixture was capable of applying 89,000 N (20,000lb) of load to the specimen. The burner has a capacity of 0.5 kg/sec (1 lb/sec) at 1900 K (3000 °F). A more detailed description of the burner may be found in reference 10.

Although holding grips were provided on each specimen to permit tensile loading to simulate centrifugal forces, tensile loading was not applied in this investigation. The specimens were clamped securely to heavy platens which were in turn connected to the loading fixture. The entire fixture pivoted so as to move the specimen in and out of the burner exhaust, (shown schematically in fig. 4). In this way, the burner could operate at steady-state while the specimen was thermally cycled between ambient temperature and 1300 K (1880°F).

The total cooling air flow rates were typical of those experienced by a first-stage turbine in an aircraft gas turbine engine. The distribution to each coolant passage was selected to provide the most uniform surface temperature possible across the blade surface. Metering orifice plates were used to control the division of cooling air to the cooling passages.

## Test Procedure

The loading fixture was pivoted by means of an electrically actuated hydraulic cylinder so as to move the specimen into and out of the burner exhaust gas stream. This is shown schematically in figure 4. The burner was brought to operating temperature with the simulated turbine blade in position out of the burner exhaust gas stream. Attached to the fixture was a platform on which the extensometer or the camera of the IRP pyrometer were mounted. The two noncontacting methods were evaluated separately under similar but not identical conditions in the thermal fatigue test rig. For the extensometer strain measurements, a thermocouple was used to measure the local blade temperature where the strain measurement was made. The temperature was recorded during the complete cycle.

For the IRP pyrometer surface temperature distribution measurement, an optical pyrometer was sighted on a fixed location in the field of view of the camera. This temperature measurement served as the reference temperature for calibrating the temperature range on the thermal image. For these tests, only heated steady state data were photographically recorded.

## RESULTS AND DISCUSSION

### Transient Strain Measurement

Figure 5 shows strains and temperatures of the mid-span region at the leading edge for the three B-1900 simulated turbine blades evaluated. Temperature was measured using a thermocouple. Strain is plotted versus temperature, with elapsed cycle time indicated along the curve. The strain values plotted were determined with the following considerations: The electro-optical extensometer measured the relative displacement of the targets at the leading edge mid-span region. Knowing the gage length, it was possible to calculate the total leading edge strain. Thermal bowing, which is usually present in cambered airfoils under thermal stress, was prevented by clamping the specimen between heavy platens. This was done in order to stabilize the specimen and also to simplify the subsequent stress analysis. The assembly which prevented thermal bowing also prevented the airfoil specimen from warping in a manner similar to an unrestrained blade to relieve thermal stress. Therefore, strain due to average uniform thermal expansion could be calculated and subtracted from the calculated total strain



value. The resulting mechanical strain is plotted in figure 5. Strain results were reproducible within 4%.

Figure 5(a) shows the strain-temperature cycle of the uncooled, solid simulated turbine blade at the mid-span leading edge. The maximum compressive strain value for the uncooled solid blade was reached after only five seconds of heating. The blade experienced compressive mechanical strain throughout the entire portion of the heating cycle. Figure 5(b) shows the cycle of the simulated turbine blade employing convection with local film cooling. As in the case of the uncooled solid blade, the leading edge maximum compressive strain was attained during the onset of the heating cycle and the strain remained compressive during this entire portion of the cycle. The strain-temperature cycle of the convection cooled blade, figure 5(c), showed less compressive strain than the other blade configurations. Compressive strain was noted only during the initial portion of the heating cycle (approximately the first three seconds), and the strain thereafter was generally tensile.

#### Surface Temperature Distribution Measurement

Temperature distribution measurements of the three blades, at heated steady state conditions, were made from thermal images taken of the heated blades. Each image was scanned with a micro-densitometer which measures the local film density of the measuring aperture. The aperture used had an equivalent spot size of 0.13 cm (0.050 in) on the blade surface.

Although temperature distributions were obtained at heated steady state conditions, they could have been done at any time during the thermal cycle. Thermal images taken at discrete times during the heating and cooling cycle were analyzed in the same manner as described for the heated steady state condition.

Typical turbine blade temperature records obtained with the densitometer are shown in figure 6. The uncooled, solid blade is illustrated in figure 6(a), the blade that was convectively cooled with local film cooling in figure 6(b), and the convection cooled blade in figure 6(c). The cross-section of each test blade is shown above each mid-span temperature profile. The contours on the surface were assigned temperatures by projecting corresponding locations from the mid-span profile scan to the contour map at the mid-span locations indicated on the figure. Generally all the contours can be calibrated from one or two profile scans. With this procedure the temperature at any point on the blade surface can be determined.

The effect of the various cooling configurations on temperature is apparent by examining the surface temperature distribution maps. The range of temperature and the severity of thermal gradients are evident in the mid-span temperature profile scans. The drop in temperature along the chord of the solid blade was observed because the test blade was in an open jet, rather than an enclosed tunnel. The burner exhaust gas flow impinged directly on the leading edge. Consequently the temperature distribution of the uncooled, solid blade (fig. 6a) in general follows the gas temperature profile. In figure 6b, the convectively cooled blade with local film cooling, showed the most severe temperature gradients. The blade cooled by convection only, showed the lowest spread of temperature over its surface, as well as the least severe temperature gradients (figure 6c). Such gradients could of course be altered by redesign of the cooling chambers to meter the cooling air differently.

#### CONCLUDING REMARKS

Noncontacting techniques to measure strain and temperature were successfully applied to three simulated turbine blades. Leading edge strain and surface temperature were obtained by cycling two cooled and one uncooled simulated turbine blade (3 minutes heating and 1 minute cooling). The blades were moved into and out of a Mach 1 hot gas stream so that metal temperatures of the blade ranging from 300 K (80 °F) to 1300 K (1880 °F) were obtained. Both the uncooled, solid blade and the convectively cooled blade with local film cooling, sustained substantial compressive mechanical strain throughout the 180 seconds of heating. The convection cooled blade showed less compressive strain than the other two blade configurations. Accuracy of the system was  $\pm 0.04$  % of the 1.47cm (0.561 in.) gage length. Strain results were reproducible within 4%. IRP pyrometry showed gross variations of surface temperature distribution for the various cooling configurations. In these tests the blade cooled by convection only showed the lowest spread of temperatures over its surface, as well as the least severe temperature gradients. Compressive strain at the mid-span leading edge was noted during the initial portion of the heating cycle for all of the blades. However, as the cooling portion of the cycle was initiated, strains tended to become tensile in nature, except for the convection cooled blade. This blade reached a peak tensile strain at the end of the heating portion of the cycle.

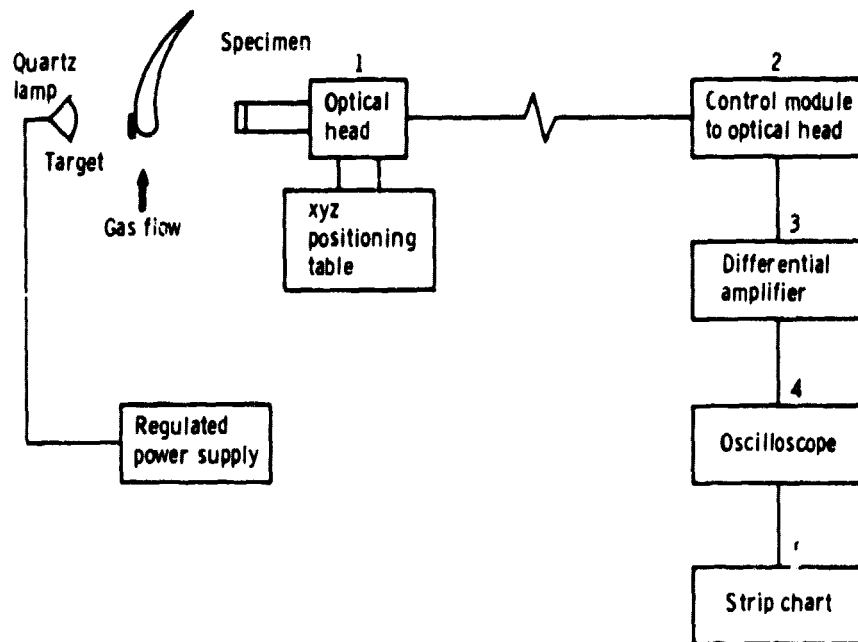
The method of strain and temperature measurement described has the potential for obtaining the accurate measurements needed in the development and evaluation of a

theory for predicting the thermal fatigue of structural components.

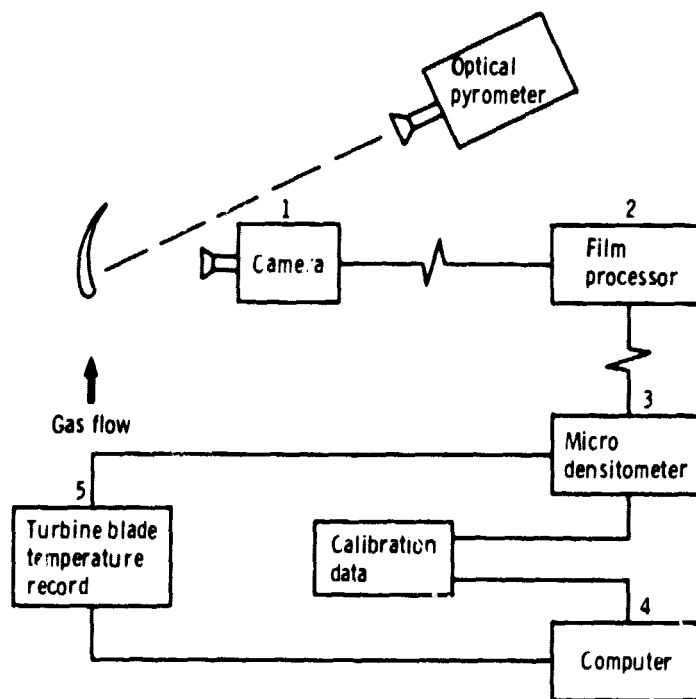
#### REFERENCES

1. Hirschberg, M. H.; and Halford, G. R.: Use of Strainrange Partitioning to Predict High Temperature Low-Cycle Fatigue Life. NASA TN D-8072, 1976.
2. Halford, G. R.; and Manson, S. S.: Life Prediction of Thermal-Mechanical Fatigue Using Strainrange Partitioning. NASA TM X-71829, 1975.
3. Hirschberg, M. H.; and Halford, G. R.: Strainrange Partitioning: A Tool for Characterizing High-Temperature Low-Cycle Fatigue. NASA TM X-71691, 1975.
4. Halford, G. R.; Hirschberg, M. H.; and Manson, S. S.: Temperature Effects on the Strainrange Partitioning Approach for Creep-Fatigue Analysis. NASA TM X-68023, 1972.
5. Manson, S. S.; Halford, G. R.; and Hirschberg, M. H.: Creep-Fatigue Analysis by Strain-Range Partitioning. NASA TM X-67838, 1971.
6. Spera, David A.; and Grisaffe, Salvatore J.: Life Prediction of Turbine Components: On-Going Studies at the NASA Lewis Research Center. NASA TM X-2664, 1973.
7. Spera, D. A.; Calfo, F. D.; and Bizon, P. T.: Thermal Fatigue Testing of Simulated Turbine Blades. NASA TM X-67820, 1971.
8. Calfo, Frederick D.; and Bizon, Peter T.: Experimentall Determination of Transient Strain in a Thermally-Cycled Simulated Turbine Blade Utilizing a Non-Contact Technique. NASA TM-73886, 1978.
9. Pollack, F. G.; and Hickel, R. O.: Surface Temperature Mapping with Infrared Photographic Pyrometry for Turbine Cooling Investigations. NASA TN D-5179, 1969.

10. Johnston, J. R.; and Ashbrook, R. L.: Oxidation and Thermal Fatigue Cracking of Nickel- and Cobalt-Base Alloys in a High Velocity Gas Stream. NASA TN D-5376, 1969.



(a) Electro-optical extensometer.



(b) Infrared photography.

Figure 1. - General diagram of strain and temperature measuring system.

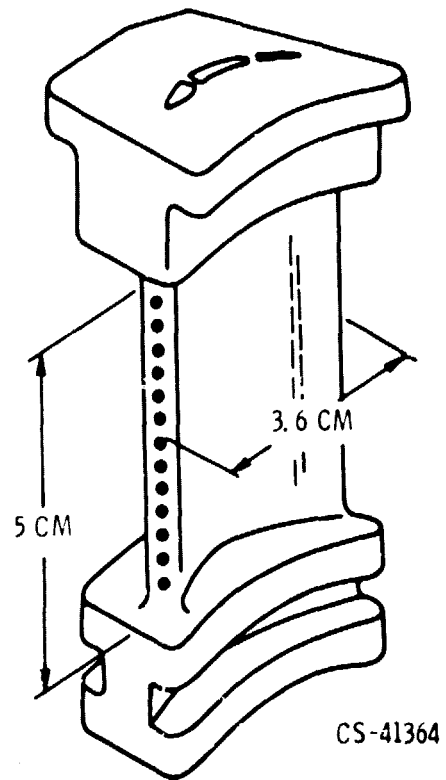
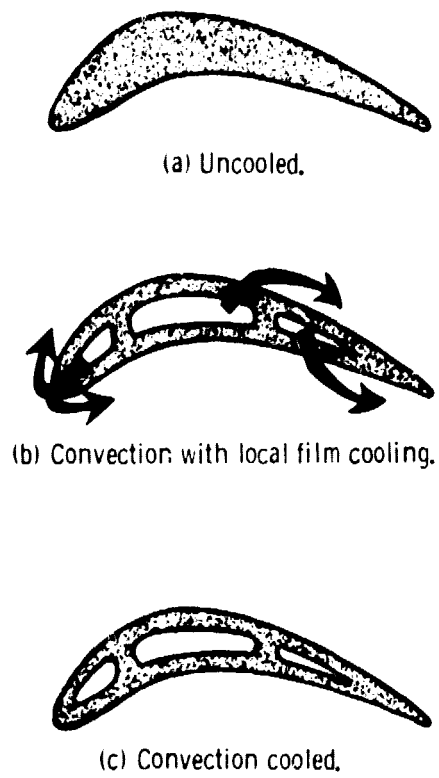


Figure 2. - Simulated turbine blades.

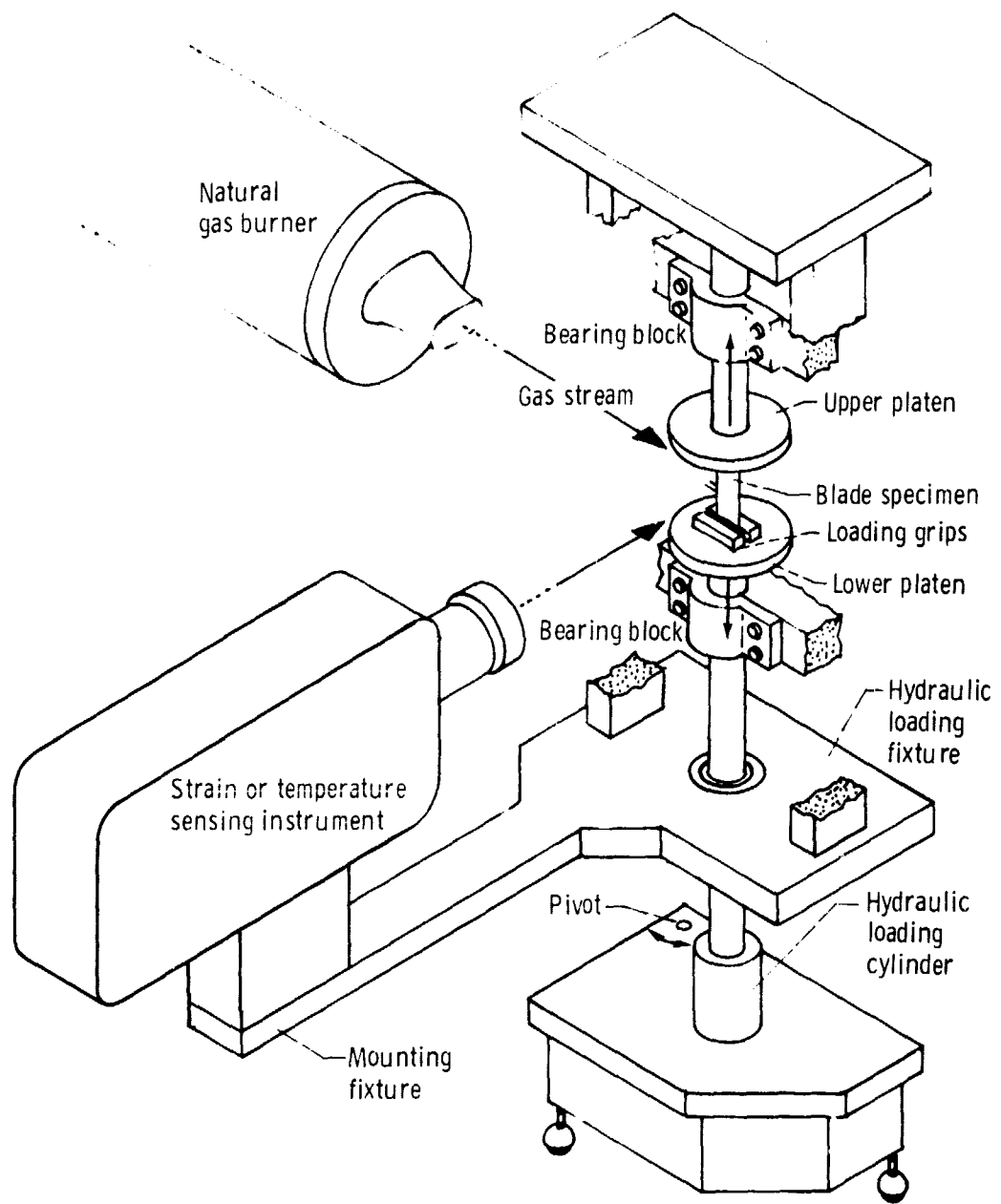


Figure 3. - Schematic of facility for thermal-fatigue testing of simulated turbine blades.

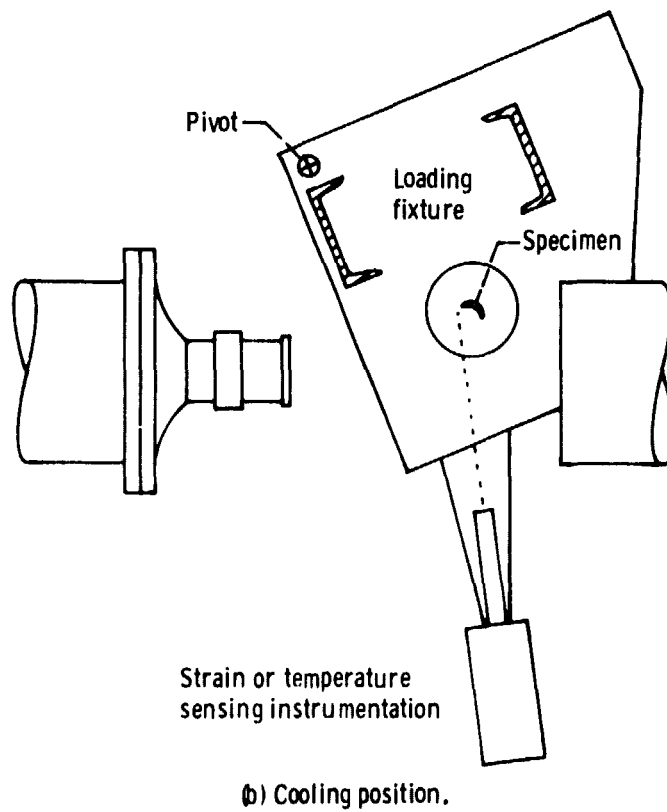
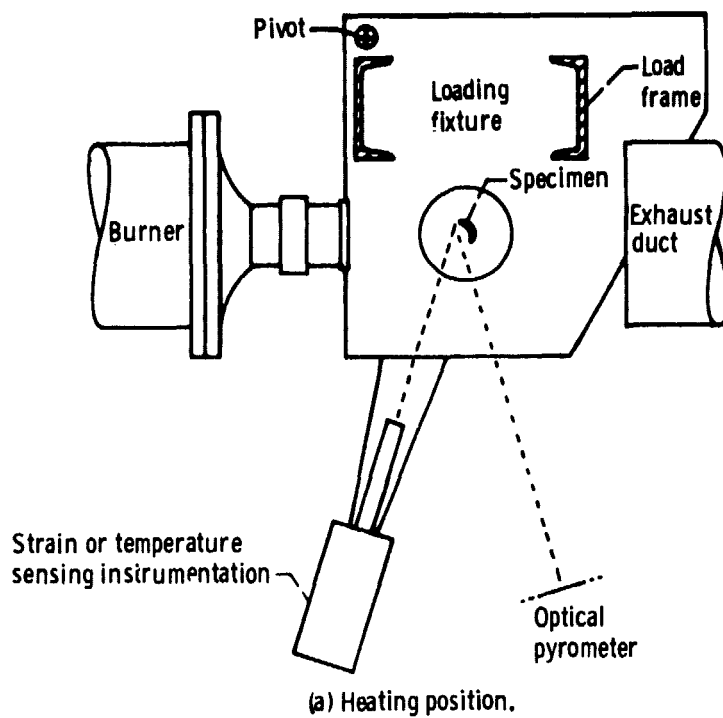
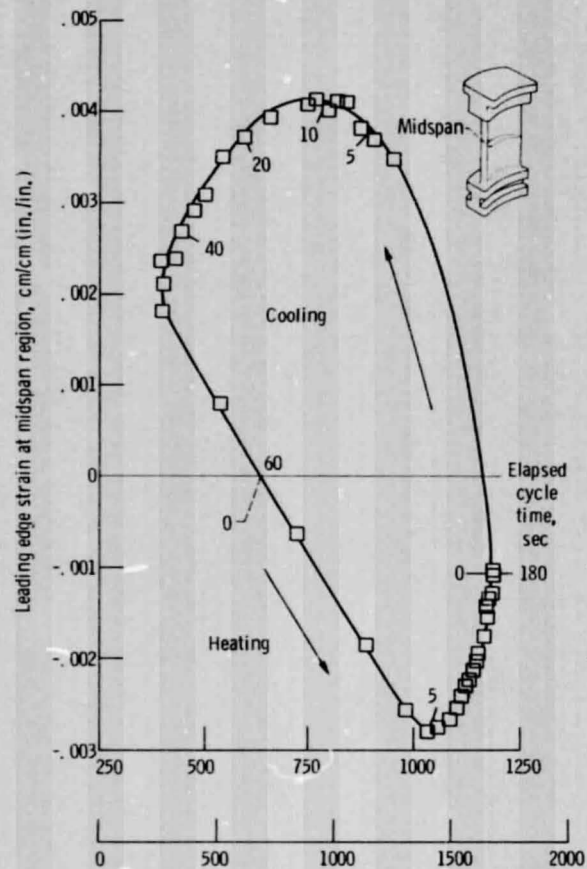
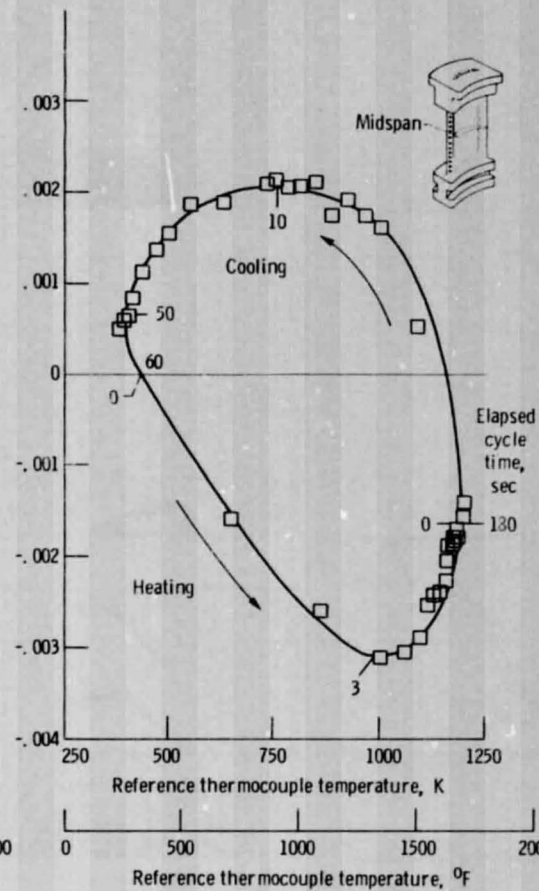


Figure 4. - Schematic of facility showing the specimen located in the heating and cooling positions.

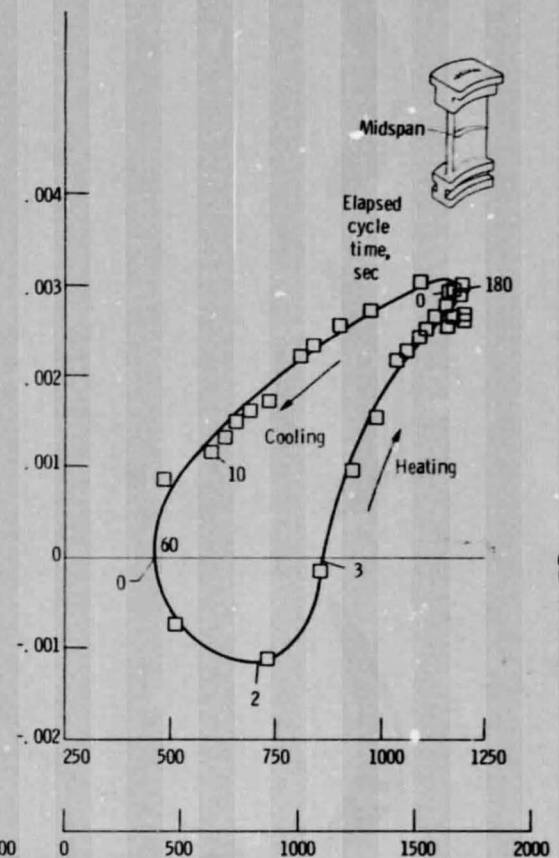




(a) Uncooled solid blade.



(b) Convection with local film cooling blade.



(c) Convection cooled blade.

Figure 5. - Strain-temperature cycle at midspan of leading edge of a B-1900 simulated turbine blade. Cycle time: 180 second heating and 60 second cooling.

ORIGINAL PAGE IS  
OF POOR QUALITY

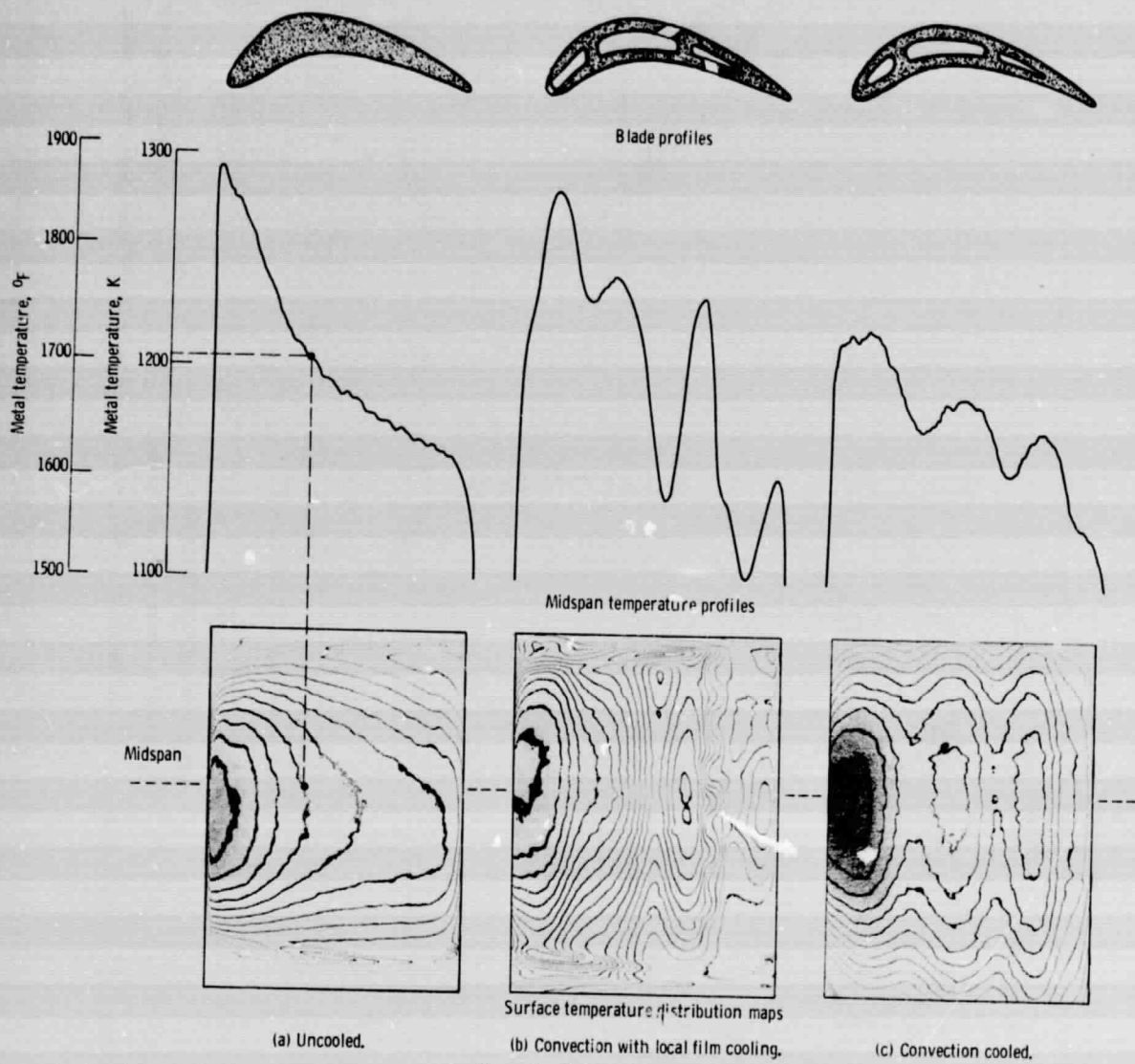


Figure 6. - Turbine blade temperature records.

ORIGINAL PAGE IS  
OF POOR QUALITY